

Optimum Conditions for the Removal of Cr(VI) using Modified Eucalyptus Bark

Fenjie Niu,^a Shuangquan Yao,^a Shuangxi Nie,^{a,b,c} Chengrong Qin,^a Hongxiang Zhu,^a and Shuangfei Wang^{a,*}

The aims of this study were response surface modeling and optimization of Cr(VI) removal from solution using formaldehyde-modified eucalyptus bark. A high removal rate of Cr(VI) was achieved under the conditions of low adsorbent dosing quantity and high initial concentration of Cr(VI). Analysis of variance showed a high multiple coefficient of determination ($R^2=0.9875$), adjusted determination coefficient ($R^2_{Adj}=0.9714$), and the good second order regression equation. The initial concentration of Cr(VI) was 40.15 mg/L, adsorbent dosing quantity 3.40 g/L, and initial reaction pH 2.78, and the largest removal rate was 99.998% under the optimum reaction conditions. Langmuir and Freundlich isothermal models described well adsorption of Cr(VI) by the modified stringy bark. Adsorption kinetics studies showed that the adsorption was controlled by multiple factors, dominated by chemical adsorption. The adsorption was found to be spontaneous and endothermic, with $\Delta G^0 < 0$, $\Delta H^0 > 0$, and $\Delta S^0 > 0$. Adsorption of Cr(VI) by formaldehyde-modified stringy bark was partly controlled by REDOX reactions. The adsorbents were characterized by SEM and FTIR.

Keywords: Response surface; Modified eucalyptus bark; Removal rate; Adsorption kinetics

Contact information: a: College of Light Industry and Food Engineering, Guangxi University, Nanning, 530004, PR China; b: Department of Chemical Engineering, University of New Brunswick, Fredericton, E3B5A3, Canada; c: The Guangxi Key Laboratory of Environmental Engineering, Protection and Assessment, Guilin 541004, PR China; *Corresponding author: wangsf@gxu.edu.cn

INTRODUCTION

Chromium and its compounds are extensively used in industry, with the most common and important sources coming from electroplating, tanning, water cooling, pulp production, dyes and pigments, film and photography, wood preservation, and alloy manufacture (Saha and Orvig 2010). In ground water and soil, chromium exists in two major oxidation states: the oxidized hexavalent chromium and the less-oxidized trivalent chromium. Trivalent chromium compounds are sparingly soluble in water, while hexavalent chromium compounds are quite soluble (Saha *et al.* 2011). Cr(III) is an essential element of mammals metabolism (Arulkumar *et al.* 2012), but Cr(VI) is toxic, carcinogenic, and teratogenic, so it is subject to strict emission controls.

There are many methods to deal with chromium metal pollution, such as chemical precipitation, ion exchange, electrochemical precipitation, reduction, and adsorption (Sahu *et al.* 2009). The absorption technique has received a lot of research attention due to its simple operation and high efficiency. The key of adsorption technology is to choose an appropriate adsorbent. Except for its relatively high price, activated carbon can be considered to be an ideal adsorbent. Many agriculture forestry by-products have been

demonstrated as good low-cost adsorbents for Cr(VI) and Cr(III) due to their widespread availability (Miretzky and Cirelli 2010). Different agricultural wastes such as bagasse and corncob have been studied relative to the adsorption of Cr(VI) under different experimental conditions (Garg *et al.* 2007); the results showed that the maximum adsorption was achieved at a pH of 2 and 60 min reaction time. Larch bark was studied for removal of Cr(VI); factors influencing the experimental results were determined, and the adsorption data was found to conform to the Langmuir and Freundlich isotherms (Aoyama and Tsuda 2001).

The development of fast-growing eucalyptus forests has been particularly fast in recent years, especially in Guangxi China. The forecasted growth rate is about 25 million m³ of eucalyptus per year through 2015, along with about 7.5 million m³ / year of eucalyptus bark in Guangxi. Its surface contains functional groups such as -COOH, -OH, and -NH₂ that can be used for adsorption of metal ions. However, the content of such groups is moderate, and hence the adsorption capacity for metal ions is limited. Sarin and Pant (2006) tested several low-cost biomaterials for removal of chromium, such as bagasse, charred rice husk, activated charcoal, and eucalyptus bark, and their results showed that eucalyptus bark had a highest chromium(VI) removal rate. In addition, the adsorption data were fitted well by the Freundlich isotherm, and the kinetic data were analyzed by using a first order Lagergren kinetic expression. It has been shown that modification with formaldehyde can effectively block the release of colorful substances from eucalyptus bark without affecting the adsorption performance in the cases considered (Sarin and Pant 2006). Although results show that eucalyptus bark can remove hexavalent chromium, a long modification time for eucalyptus bark may undermine its content of organic functional groups and affect its adsorption efficiency. The present work considers the use of formaldehyde-modified eucalyptus bark as an adsorbent to study the adsorption characteristics of Cr(VI), not only ensuring the adsorption effect, but also greatly reducing the modification time. The changes of the reaction conditions are crucial for the adsorption process. Studies of individual influencing factors are widely employed, but they are not the best way to study the interaction effects between all the influence factors in an adsorption process. Response Surface Methodology has been used to assess the relative importance of influencing factors, ultimately determining the optimal operating conditions for adsorption of metal ions (Shojaimehr *et al.* 2014). A design with three levels was employed in this work, based on the following three factors affecting the adsorption: the initial Cr(VI) concentration, the pH, and the quantity of adsorbent employed. The adsorption kinetics and thermodynamics under the optimum operating conditions were studied, respectively, in order to further investigate the Cr(VI) adsorption process. The reaction mechanism was considered in light of results from FTIR, SEM-EDS, and ICP analyses.

EXPERIMENTAL

Adsorbate

1000 mg/L K₂Cr₂O₇ stock was prepared from guaranteed reagent K₂Cr₂O₇ after drying for 2 h at 120 °C, followed by dissolution in deionized water. The stock solution was diluted with deionized water according to certain proportions, in accordance with the experiment concentrations of 30 mg/L to 50 mg/L.

Adsorbent

Pretreatment of eucalyptus bark

Before adsorption of hexavalent chromium, the fly ash on the surface and the more easily dissolved coloring matter should be removed from eucalyptus bark through simple pretreatment, so as not to affect the adsorption effect. The procedure used for initial treatment of the bark is summarized in Fig. 1. Eucalyptus bark was smashed with a pulverizer after drying, which is called “breaking” in Fig. 1. After the pretreatment, eucalyptus bark was sealed and packaged for the dryer.

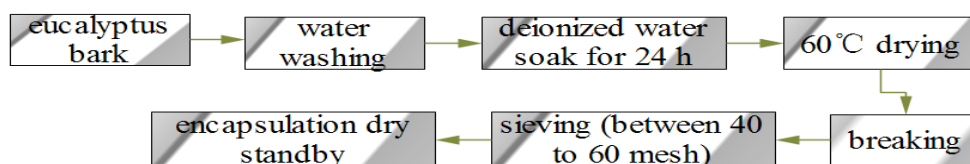


Fig. 1. Procedure used for initial washing, drying, diminution, and sieving of eucalyptus bark

Formaldehyde modified eucalyptus bark

100 mL of 0.1 mol/L hydrochloric acid solution, 5 mL of formaldehyde solution (40%), and 3 g of pretreated eucalyptus bark were added to a 250 mL three stoppered flask, stirring gently 3 h at 60 °C thermostat water bath, and filtering after stirring. Eucalyptus bark was dried to constant weight at 60 °C (Sarin and Pant 2006) after washed with deionized water until neutral pH was measured.

Activation of powder activated carbon

Comparison data were obtained for the removal of Cr(VI) using activated carbon as the control group. Activated carbon was prepared using the following processing steps:

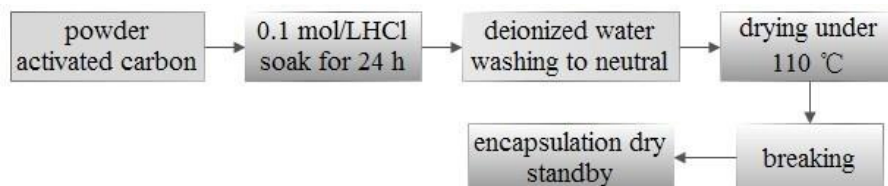


Fig. 2. Steps used in preparation of the activated carbon for comparative tests

Static Adsorption Experiments

The selected amounts of eucalyptus bark and 100 mL of a certain concentration of Cr(VI) solution were added to the 250 mL conical flask, adjusting the initial pH of the solution (0.1 mol/L HCL and NaOH to adjust), shaking the flask for 2 h at a constant temperature at 30 °C and 150 rpm. The mixture was then filtered and the concentration of Cr(VI) in the filtrate was evaluated using the "diphenylcarbazide spectrophotometric method". Each test was repeated three times to obtain an average. The Cr(VI) adsorption rate and adsorption capacity were calculated as follows,

$$R(\%) = \frac{C_i - C_e}{C_i} \times 100 \quad (1)$$

$$q_e = \frac{V(\rho_1 - \rho_2)}{m} \quad (2)$$

where R is the adsorption extent of Cr(VI), C_i is the initial Cr(VI) concentration (mg/L), C_e is the Cr(VI) concentration after equilibration (mg/L), q_e is the adsorption capacity (mg/g), V is the sample volume (L), ρ_1 is the initial concentration of sample (mg/L), ρ_2 is the concentration of sample after equilibration (mg/L), and m is the adsorbent quantity employed (g).

Response Surface Design

RSM statistical methods, the regression model equation, and operating conditions were determined using an experimental approach related to that used by Alam *et al.* (2007). A Box-Behnken design (BBD) was used. BBD is a kind of RSM often used to study the influence of the test factors and response value, with accurate determination of the relationship between influence factors and the response values (Nie *et al.* 2013). A BBD central composite Design method was applied in this experiment, with the Cr(VI) adsorption rate as the response value Y . The experimental design involved three factors and three levels for the three important factors of influencing the Cr(VI), for instance, initial reaction concentration of hexavalent chromium, adsorbent dosage, and pH. Design Expert V8.0.6.1 software was used as the fitting system to seek the optimal value. Factor levels are shown in Table 1.

Table 1. BBD Experiment Factors Level Table

Level	Factors		
	A Concentration /mg.L ⁻¹	B Dosage /g	C pH
-1	30	0.2	2
0	40	0.3	3
1	50	0.4	4

Characterization of Adsorbent

The adsorbent was characterized by SEM-EDS and FTIR, observation of morphology, and semi-quantitative analysis of adsorbent with or without adsorption by SEM-EDS (Hitachi S-3400N). The FTIR tests employed the KBr tableting method under analysis conditions of 16 scans at a resolution of 4 cm⁻¹ measured between 500 and 4,000 cm⁻¹.

RESULTS AND DISCUSSION

Removal of Cr(VI) with Similar Adsorbents

Table 2 shows the comparison of adsorption ability for the three adsorbents. The concentration of Cr(VI) was determined by static adsorption experiment. Eucalyptus bark, formaldehyde-modified eucalyptus bark, and activated carbon were evaluated under the same conditions, which were an adsorbent dosing amount of 0.3 g, an initial Cr(VI) concentration of 20 mg/L, 30 °C constant temperature oscillation with 90 min, and an initial reaction pH of 3. Eucalyptus bark exhibited good adsorption of Cr(VI) after a simple preprocessing, although higher removal of Cr(VI) was achieved by the activated carbon (Table 2). Thus, the unmodified eucalyptus bark had better adsorption performance with low concentration hexavalent chromium. Although its adsorption performance was good,

it did not have high enough efficiency to meet the demands for large-scale use. The Cr(VI) removal value increased from 80.4% to 96.7% after formaldehyde modification, which was a slightly higher value than was obtained with the activated carbon. The supernatant solution after the simple pretreatment of eucalyptus bark was observed to be slightly yellow, whereas in the cases of formaldehyde-modified eucalyptus bark and activated carbon, the supernatant was colorless. These findings showed that the formaldehyde crosslinking not only resulted in higher adsorption efficiency, but it also effectively prevented the dissolution and release of colorful substances from the bark, increasing the transparency of the filtrate, and reducing the follow-up measurement error.

Table 2. Comparison of Adsorption Ability

Adsorbent	A	Cr (VI) concentration (mg·L ⁻¹)	Removal (%)
Eucalyptus bark	0.213	3.913	80.44
Formaldehyde-modified bark	0.036	0.655	96.73
Activated carbon	0.048	0.876	95.62

Response Surface Methodology

Regression model equation

A quadratic model was selected according to software recommended. The experimental design and results are shown in Table 3. The experimental results were fitted using multivariate regression. Variance analysis was carried out, with the adsorption as the response value Y. The quadratic regression equation for the best fit was (Zhang *et al.* 2010):

$$Y = 99.41 + 1.25A - 1.56B + 3.56C + 0.6AB - 2.12AC + 3.36BC - 0.05A^2 - 0.92B^2 - 3.41C^2 \quad (3)$$

Table 3. BBD Experimental Model and the Response Values Results

No.	Factors			Adsorption, Y(%)
	A(mg.L ⁻¹)	B(g)	C	
1	30.00	0.30	4.00	96.46
2	40.00	0.30	3.00	99.56
3	50.00	0.30	2.00	99.98
4	30.00	0.30	2.00	98.01
5	40.00	0.40	4.00	97.17
6	40.00	0.30	3.00	99.58
7	40.00	0.30	3.00	99.54
8	40.00	0.30	3.00	99.56
9	40.00	0.40	2.00	97.70
10	30.00	0.40	3.00	99.97
11	40.00	0.20	4.00	86.05
12	40.00	0.20	2.00	100
13	40.00	0.30	3.00	99.55
14	30.00	0.20	3.00	98.41
15	50.00	0.30	4.00	89.94
16	50.00	0.40	3.00	99.97
17	50.00	0.20	3.00	96.01

Statistical analysis

Analysis of variance (ANOVA) is shown in Table 3. According to the ANOVA, the F-value was 61.41. Prob (P) which was greater than the F value (< 0.0001), indicating that the model was highly significant. The multiple coefficient of determination R^2 was 0.9875, indicating that the correlation was good. The adjusted determination coefficient R^2_{Adj} was 0.9714, indicating that the variability of 97.14% of experimental data can be explained in the regression model. The CV value, 0.76%, indicated that the reliability and accuracy of the experiment was very good. Adeq precision is the ratio of effective signal and noise, for which a value greater than 4.0 is considered to be reasonable (Sahu *et al.* 2009). The adeq precision of the experiment was 27.6. In conclusion, a suitable model for Cr(VI) adsorption was provided by the regression equation. The factors A, B, and C were each found to be significant for the adsorption effect, as shown in Table 4. The squared terms B^2 and C^2 were significant for the adsorption effect. The interactive terms AC and BC were profoundly important relative to adsorption. The experiment value and the predicted value of Cr(VI) adsorption rate are shown in Fig. 3.

Table 4. Analysis of Variance

Source	Sum of Squares	df	Mean Square	F Value	p-value Prob > F	Significance
Model	235.59	9	26.18	61.41	< 0.0001	significant
A	4.19	1	4.19	9.83	0.0165	significant
B	6.51	1	6.51	15.27	0.0058	significant
C	11.80	1	11.80	27.68	0.0012	significant
AB	1.44	1	1.44	3.38	0.1087	
AC	18.02	1	18.02	42.27	0.0003	significant
BC	45.02	1	45.02	105.62	< 0.0001	significant
A ²	0.011	1	0.011	0.025	0.8790	
B ²	3.55	1	3.55	8.32	0.0235	significant
C ²	48.97	1	48.97	114.87	< 0.0001	significant
Residual	2.98	7	0.43	—	—	—
Lack of Fit	2.98	3	0.99	4519.81	< 0.0001	significant
Pure Error	8.800×10^{-4}	4	2.200×10^{-4}	—	—	—
Cor Total	238.57	16	—	—	—	—

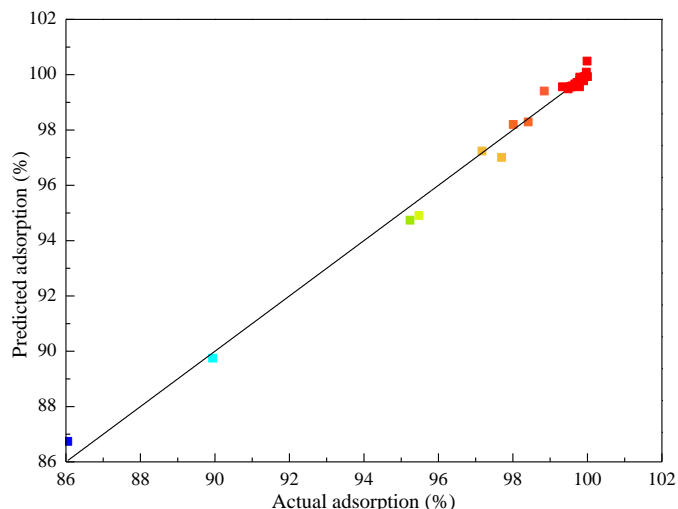


Fig. 3. Cr(VI) adsorption actual value and predictive value contrast

Cr(VI) adsorption capacity analysis

Figure 4 shows the response surface for Cr(VI) initial concentration and adsorbent additive quantity relative to the removal rate when pH is 3. As shown, the removal rate first increased and then was stable with the increase of dosing quantity under conditions of specified initial concentration. The increase of removal rate moderated slightly with the increase of dosing quantity when suitably increasing the initial concentration. Under the invariable initial concentration, when the adsorbent dosage was smaller, the adsorption was achieved easily up to the point of adsorption saturation, beyond which there was not enough adsorbent to adsorb the hexavalent chromium ion present in the solution. When the additive quantity was increased, more active functional groups were made available, and these also provided a larger surface area for the adsorption of hexavalent chromium. Meanwhile the removal rate showed a rising trend. But when the amount of adsorbent was increased to a certain degree, the amount of hexavalent chromium became the limiting factor; this means that some of the functional groups on the adsorbent were not occupied, and the removal rate became stable.

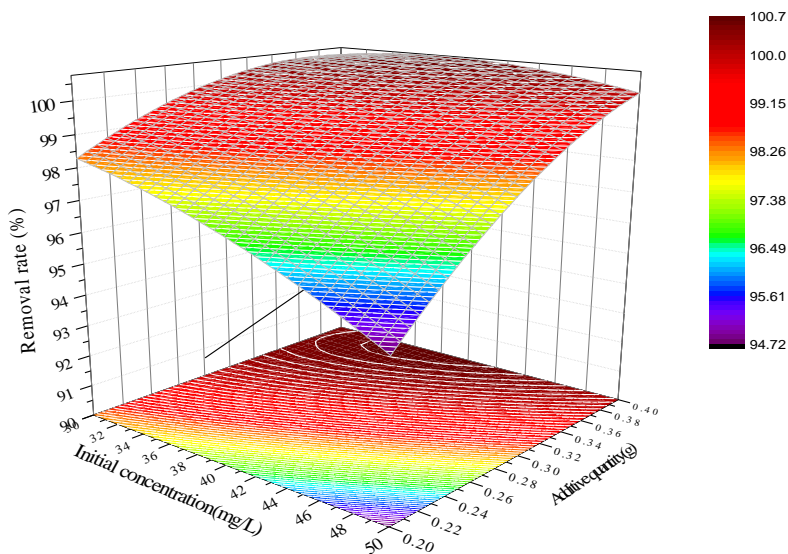


Fig. 4. Initial concentration and additive quantity on influence of the removal rate (pH=3)

Figure 5 shows the influence of Cr(VI) initial concentration and pH on the removal rate when adsorbent dosing quantity was 0.3 g. When the Cr(VI) initial concentration was 30 to 35 mg/L, the removal rate was increased with the decreasing of reaction pH. When the initial concentration was increased to the range 35 to 45 mg/L, the removal rate was increased slightly with the decreasing of the reaction pH. Because pH influences the protonation degree of eucalyptus surface, a lower pH can increase the protonation degree, leading to a stronger adsorption capacity for Cr(VI). However, with the increase of pH, the protonation degree of the eucalyptus surface is reduced, leading to a weaker attraction of Cr(VI). As a result, the removal rate increases as the pH decreases when the initial concentration was 30 to 35 mg/L. When the initial concentration was increased from 35 to 45 mg/L, the removal rate increased with the reduction of reaction pH, although the extent of increase was slightly smaller. This is because pH is more significant for the influence of the adsorption removal rate in the interaction process of all the influence factors. So a higher removal rate can be achieved when the initial concentration of Cr(VI) is appropriately increased when pH is kept at a lower level.

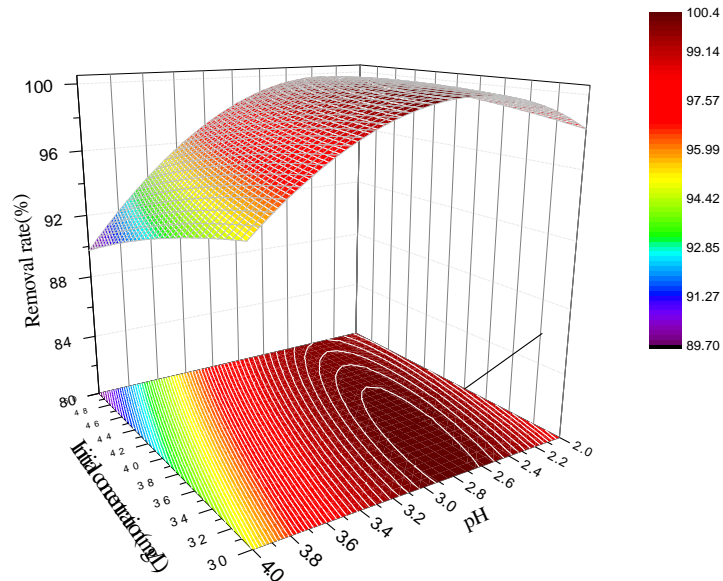


Fig. 5. Initial concentration and pH on influence of the removal rate (additive quantity 0.3 g)

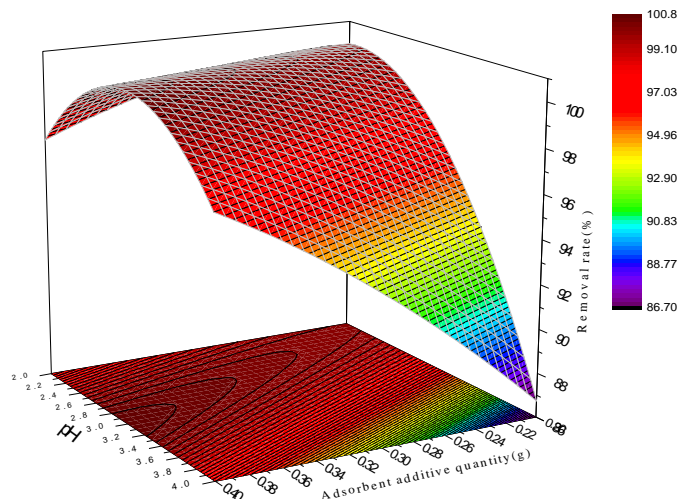


Fig. 6. pH and dosing quantity on influence of the removal rate (initial concentration 40 mg/L)

Figure 6 shows the influence of pH and additive quantity on the removal rate when Cr(VI) initial concentration was 40 mg/L. The removal rate of Cr(VI) was increased with the decreasing of pH when the adsorbent dosing quantity was 0.20 to 0.30 g. When the added quantity was increased suitably, the removal rate of Cr(VI) was increased more obviously with the decreasing of pH. When the initial concentration was held constant, the increase of adsorbent dosage and low pH, which can increase the degree of protonation of the adsorbent surface, can allow more of the hexavalent chromium to be adsorbed effectively and faster. So the removal rate rises. Thus, in order to obtain a higher removal rate of Cr(VI), the pH should be kept at lower levels and adsorbent additive quantity should be increased slightly.

Optimization of the model

The main purpose of modeling is to find the optimal process of maximum Cr(VI) removal rate by use of a suitable equation. The optimal process conditions were Cr(VI)

initial concentration of 40.15 mg/L, adsorbent dosing quantity 0.30 g, and reaction pH 2.78. The predicted removal rate was 100.4% under the optimum process parameters. The prediction value shows that the removal rate was optimal under the optimum technological parameters.

However, the predicted value was more than 100%, which means that after all hexavalent chromium was adsorbed, surplus groups or more surface area can be used to adsorb ions under the optimum technological parameters. In order to validate the accuracy and reliability of the model, a confirmatory experiment is done. As shown in Table 5, the actual Cr(VI) removal rate was 99.998%, which was very close to the predicted value 100.4%. The BBD experiment design achieved high accuracy and reliability for the removal of Cr(VI) ion in waste water.

Table 5. Confirmatory Experiment

Concentration, A(mg/L)	Dosing quantity, B(g/L)	pH, C	Cr(VI) removal rate, Y(mg/L)	
			Predicted value	Actual value
40.15	3.00	2.78	100.373%	99.998%

The Adsorption Process Research

Isothermal adsorption model research

The commonly used isothermal adsorption models are,

$$\text{Langmuir isotherm: } \frac{1}{q_e} = \frac{1}{bC_e q_m} + \frac{1}{q_m} \quad (4)$$

$$\text{Freundlich isotherm: } \ln q_e = \ln K_f + \frac{\ln C_e}{n} \quad (5)$$

where q_e is the equilibrium adsorption quantity (mg/g), C_e is the Cr(VI) concentration in the solution at equilibrium (mg/L), q_m is the maximum removal extent (mg/g), and b and K_f are constants. According to Şengil *et al.* (2009), more favorable adsorption results are shown by higher values of the constant b value in the Langmuir equation and n in the Freundlich equation.

RSM experiment results showed that Cr(VI) adsorption was most favorable, with a removal rate of 99.998% when the Cr(VI) initial concentration was 40.2 mg/L, the reaction pH was 2.78, and the adsorbent dosing quantity was 3 g/L. During isothermal adsorption modeling, the initial Cr(VI) concentration was in the range of 40 mg/L to 140 mg/L. Results for the two types of isotherms are shown in Figs. 7 and 8. Fitting results are listed in Table 6. As can be seen from Table 6, R^2 values of the Langmuir and Freundlich isothermal models were 0.98369 and 0.98612, respectively.

Both the Langmuir and Freundlich isothermal models were able to describe the adsorption of Cr(VI), and the coefficients of determination were similar in value. Thus, one cannot clearly judge whether or not the adsorption of Cr(VI) involved monolayer interactions with homogeneous or heterogeneous surface sites (Chen *et al.* 2010). However, the constants n and b value were relatively high, indicating that the strength of the adsorption process was relatively large. High q_m showed that eucalyptus bark can be very effective for hexavalent chromium removal.

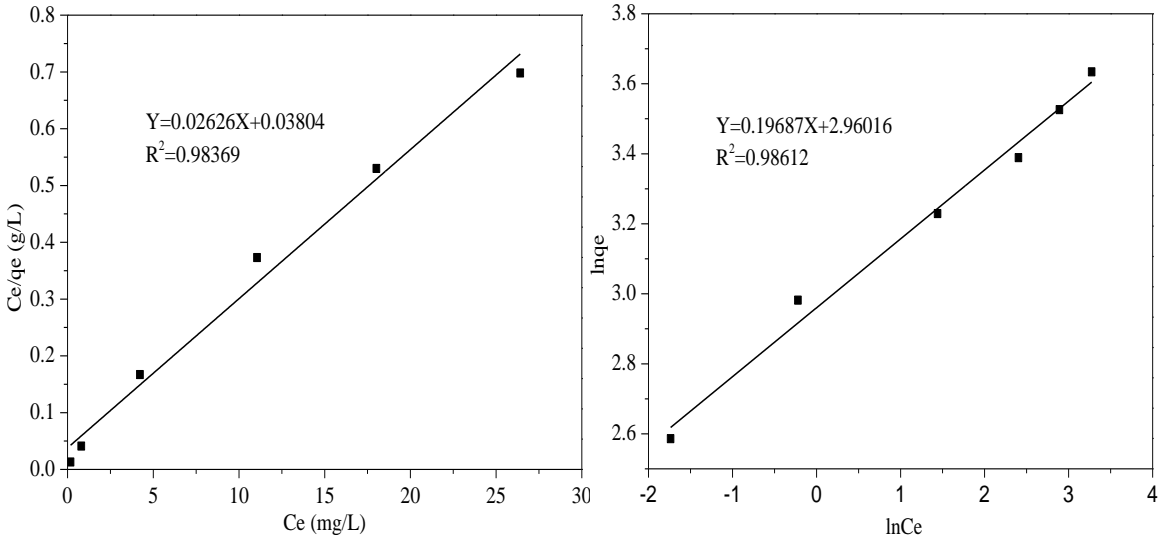


Fig. 7. Linear Langmuir isotherm adsorption Fig. 8. Linear Freundlich isotherm adsorption

Table 6. Adsorption Isotherm Fitting Results

Adsorption isotherm	Equation	Parameters
Langmuir	$\frac{C_e}{q_e} = 0.02626C_e + 0.03804$	$q_m=38.081, b=0.6903, R^2=0.98369$
Freundlich	$\ln q_e = 0.19687 \ln C_e + 2.96016$	$K_f=19.301, n=5.080, R^2=0.98612$

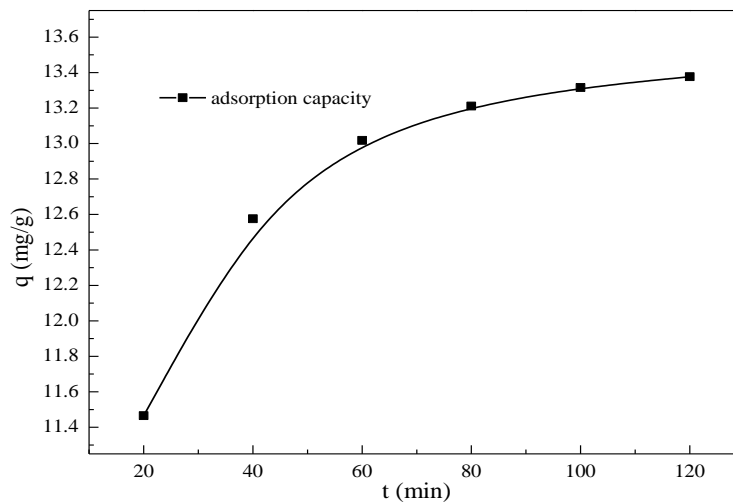


Fig. 9. Adsorption kinetics curves

Adsorption kinetics research

Figure 9 shows the adsorption kinetics curve that was obtained for the adsorption capacity q (mg/g) as a function of the adsorption time t (min). It can be seen that the rate which eucalyptus bark adsorbs Cr(VI) was rapid within the first 40 min, but the adsorption rate was reduced as reaction time increased. Adsorption rate tends to decrease in the course of adsorption. The adsorption equilibrium was almost reached at 120 min, and adsorption capacity of Cr(VI) was judged to be 13.4 mg/g.

In order to better analyze adsorption kinetics of modified eucalyptus bark for Cr(VI) removal, the adsorption kinetic data were respectively fitted by pseudo-first-order and pseudo-second-order adsorption kinetics equations,

$$\frac{1}{q_t} = \frac{1}{q_e} + \frac{K_1}{q_e t} \quad (6)$$

$$\frac{t}{q_t} = \frac{1}{K_2 q_e^2} + \frac{t}{q_e} \quad (7)$$

where K_1 is the pseudo-first-order adsorption rate constant (min), and K_2 is the pseudo-second-order adsorption rate constant (min).

Fitting results are shown in Figs. 10 and 11, as well as in Table 7. From the linear coefficients of determination 0.99532 and 0.99998 for pseudo-first-order kinetics and the pseudo-second-order kinetics models in Table 7, it is clear that the fits were good, especially for the pseudo-second-order kinetics model, which was close to 1. The linear coefficient of determination showed that the Cr(VI) adsorption process of modified eucalyptus bark could be well described by either the pseudo-first-order or the pseudo-second-order dynamic model. Though these findings could not discriminate between the two models, one can expect that the Cr(VI) adsorption process of modified eucalyptus bark is a multi-factor control process, for which the adsorption reaction rate is controlled mainly by membrane diffusion and chemical action, and it is dominated by chemical adsorption.

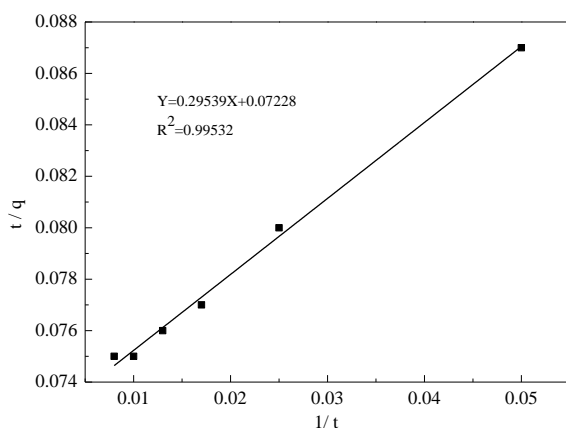


Fig. 10. First-order adsorption kinetics equation

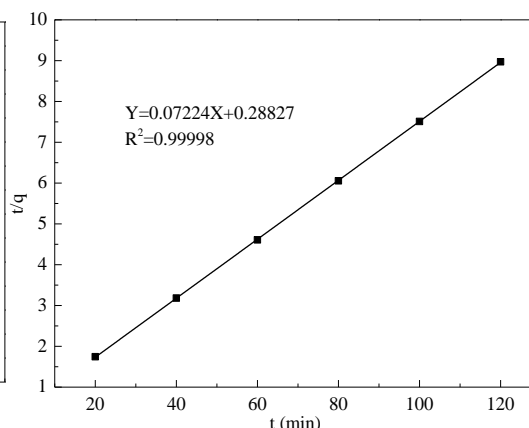


Fig. 11. Second-order adsorption kinetics equation

Table 7. Kinetic Equation Curve Fitting Results

Kinetic model	Equation	Parameters
First-order adsorption kinetics equation	$\frac{1}{q_t} = 0.29539 \times \frac{1}{t} + 0.07228$	$q_e=13.83509, k_1=4.0868$ $R^2=0.99532$
Second-order adsorption kinetics equation	$\frac{t}{q_t} = 0.07224t + 0.28827$	$q_e=13.8428, k_2=0.0181,$ $R^2=0.99998$

Adsorption thermodynamics research

In order to determine thermodynamic parameters, different temperature values for adsorption of Cr(VI) were used. Thermodynamic parameters standard Gibbs free energy change (ΔG^0), enthalpy (ΔH^0), and entropy change (ΔS^0) were evaluated as criteria by which to judge the feasibility of the adsorption process (Giri *et al.* 2012). The thermodynamic equations are as follows,

$$\Delta G^0 = -RT \ln K_c \quad (8)$$

$$\Delta G^0 = \Delta H^0 - T \Delta S^0 \quad (9)$$

$$\ln K_c = -\frac{\Delta H^0}{RT} + \frac{\Delta S^0}{R} \quad (10)$$

$$K_c = \frac{q_e}{C_e} \quad (11)$$

where ΔG^0 is the standard Gibbs free energy change (kJ/mol), R is the gas molar constant 8.314, J/(mol. K), T is the absolute temperature (K), ΔH^0 is the the standard enthalpy change (kJ/mol), and ΔS^0 is the standard entropy change (J mol⁻¹K⁻¹).

The temperature range was from 20 to 70 °C. The values of the parameters calculated are recorded in Table 8. In Table 8, $\Delta G^0 < 0$ and smaller ΔG^0 values indicates that the adsorption process was spontaneous with a good adsorption effect. The absolute value of ΔG^0 increased as temperatures rose, which showed that the rise of temperature was conducive to the adsorption (Giri *et al.* 2012). The fact that ΔH^0 was greater than zero indicates that the adsorption process was an endothermic reaction, and it was shown that the rise of temperature can effectively promote the positive reaction of adsorption. The relationship $\Delta S^0 > 0$ shows that the randomness of the liquid-solid interface is increased in the adsorption process, suggesting the possibility of a good adsorption. Therefore, the nature of Cr(VI) adsorption was a spontaneous and endothermic process. Our conclusion is consistent with the present study conclusion (Saha *et al.* 2013; Saha *et al.* 2014).

Table 8. Cr(VI) Adsorption Thermodynamic Parameters

		ΔG^0 (kJ.mol ⁻¹)					ΔH^0 (kJ.mol ⁻¹)	ΔS^0 (J.mol ⁻¹ .k ⁻¹)
20°C	30°C	40°C	50°C	60°C	70°C			
-	-	-	-	-	-	43.7658	0.19388	
11.839	16.266	17.677	18.242	20.919	22.506			

Mechanistic Research

FTIR analysis

Figure 12 shows that the FTIR spectrum of eucalyptus bark was not much different with or without adsorption of Cr(VI). Some characteristic peaks such as 3421.19 cm⁻¹ hydroxyl stretching vibration absorption peak and 2343.29 cm⁻¹ and 2360.97 cm⁻¹ amine absorption peaks appeared to experience a slight weakening, and the strength of some characteristic peaks were reduced and skewed slightly in the fingerprint region nearby. These findings indicate that the main composition of the eucalyptus bark did not experience a big change before and after adsorption. The change of characteristic peaks might be attributable to the acidic environment (pH = 2.78) or to the presence of strong oxidizing substances such as potassium dichromate in the adsorption process. The oxidation of the biomass and reduction of the Cr species may promote the adsorption of Cr(III) to freshly created carboxylic acids sites on the eucalyptus bark. If the reaction is purely an oxidoreduction reaction, some new absorption peak should appear on FTIR after adsorption. Perhaps if it is a purely physical adsorption, the obvious skewing phenomenon should appear on FTIR after adsorption, but there were only small offsets. The spectra did

not show new absorption peaks, nor obvious skewing. Although this study cannot rule out the oxidoreduction reaction, there was no clear evidence from the spectra that such effects would have a significant effect on adsorption.

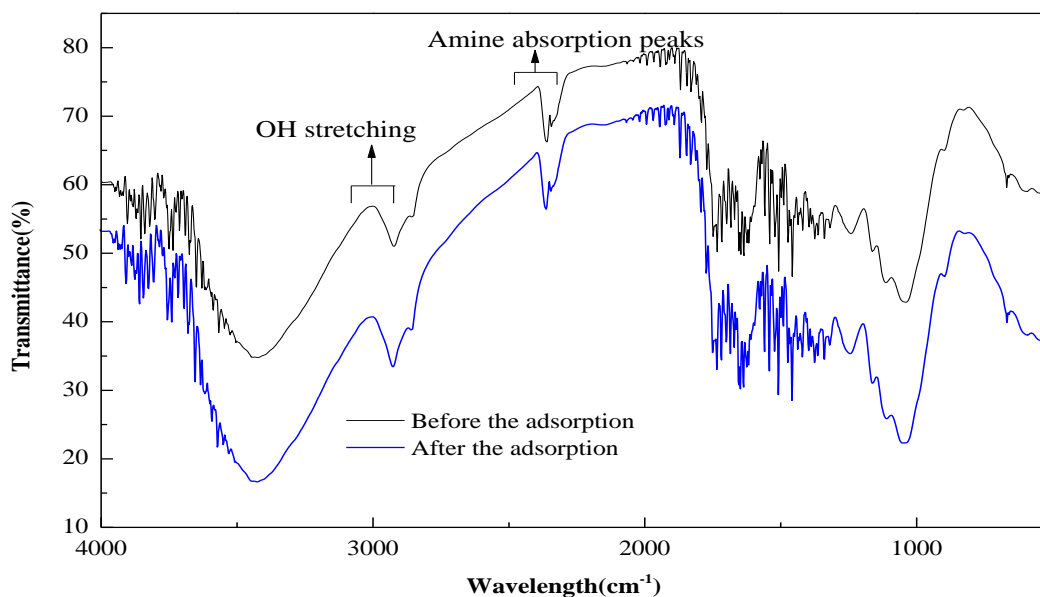


Fig. 12. FTIR analysis of adsorption

SEM-EDS analysis

Figure 13 shows SEM images of the modified eucalyptus bark with or without the adsorption of Cr(VI). As shown, the modified eucalyptus bark exhibited fiber bundles of layering and spalling. Before adsorption, the outer fiber bundles appeared relatively loose to provide a larger surface area for the adsorption of Cr(VI). After adsorption of Cr(VI) on the eucalyptus bark had taken place, there were some changes, such as blurred edges and relatively smooth surface, and the surface of eucalyptus bark appeared to be covered with a lot of sediment, making the contour fuzzy. This may possibly be caused by oxidoreduction reaction taking place on the eucalyptus skin under the acidic conditions.

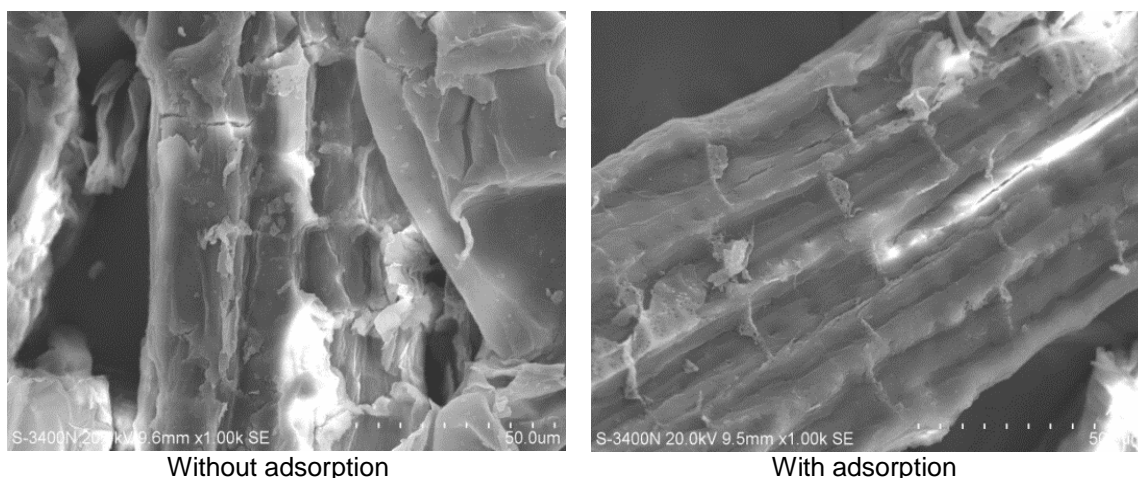


Fig. 13. SEM figure of modified eucalyptus bark in adsorption anteroposterior for Cr(VI)

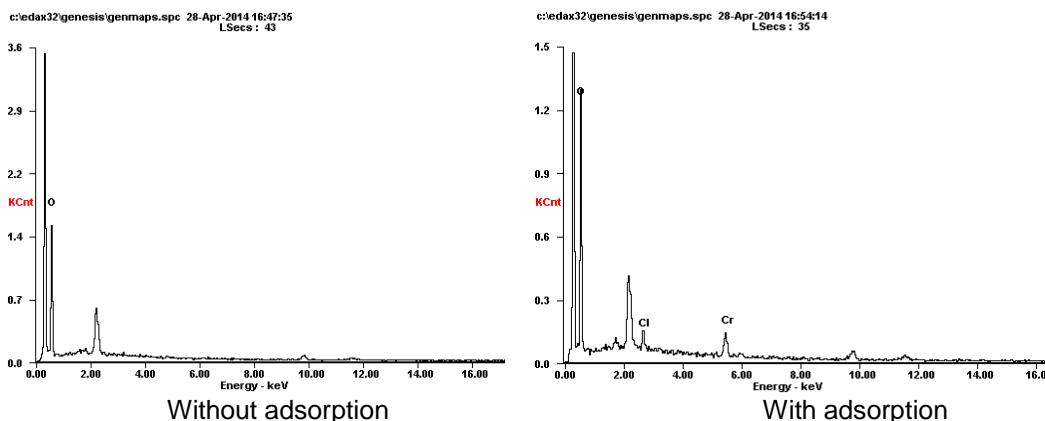


Fig. 14. EDS figure of modified eucalyptus bark in adsorption anteroposterior for Cr (VI)

In order to further study the adsorption of Cr(VI) with modified eucalyptus bark, an energy dispersive spectrometer (EDS) was employed in the experiment at the same time, and the result is shown in Fig. 14. Chromium was nonexistent before the adsorption, as shown in Fig. 14, but a lot of chromium was evident after adsorption. This indicates that Cr had been adsorbed to the surface of the adsorbent. Oxidation would be expected to render the eucalyptus bark surfaces more negative in charge, favoring the adsorption of Cr(III), which is consistent with previous research (Hubbe *et al.* 2011). However, SEM-EDS is only used to analyze the adsorption mechanism semiquantitatively; other methods are still needed for further verification.

Mechanism analysis about removal of Cr(VI) in water

In order to further validate the findings with respect to possible reduction of Cr(VI) to Cr(III), in the optimal process of Cr(VI) with an initial concentration 40.2 mg/L, an adsorbent dosing quantity of 0.30 g, a pH of 2.78, at 30 °C, and with a reaction time of 120 min, the change of Cr valence state was tested as a function of reaction time. The amount of Cr was measured using ICP. Cr(III) was determined by the difference in values between the amount of Cr and Cr(VI). Results are shown in Fig. 15. As shown, a substantial amount of reduction of the Cr(VI) was observed. Cr(III) was formed in the process of adsorption. It is understood that as the adsorption process continues, the amounts of Cr, Cr(VI), and Cr(III) tend to be stable in the solution. When reaching the reaction equilibrium, the content of Cr(VI) tends to 0 mg/L in the solution, and the content of total Cr is equivalent to Cr(III) in the solution. This is because a large proportion of the Cr(VI) is reduced to Cr(III). Organic matter of eucalyptus bark can also be oxidized by reaction with $\text{Cr}_2\text{O}_7^{2-}$ under acid conditions (Wang *et al.* 2008). It is suggested that such reactions may be associated with the observed changes in appearance, making the edges of eucalyptus bark blurred and the surface relatively smooth. Further research may be needed to solidify and to better understand this finding.

Combining with the above research, it can be seen that the nature of hexavalent chromium adsorption was a spontaneous, endothermic process when using the modified eucalyptus bark. The adsorption appeared to involve a monolayer and a heterogeneous surfaces process. The Cr(VI) adsorption process of modified eucalyptus bark was revealed to be a multi-factor controlled process, for which the adsorption reaction rate was controlled mainly by membrane diffusion and chemical action, and it was dominated by chemical adsorption. When the eucalyptus bark adsorbed hexavalent chromium, part of

hexavalent chromium was directly adsorbed onto the surface of the modified eucalyptus bark, and the rest was reduced to low-toxic trivalent chromium through the REDOX reaction to achieve the goal of removing hexavalent chromium. Although REDOX reaction exists in the process, adsorption is still basically prior, and the adsorption is not a simple chemical or physical adsorption.

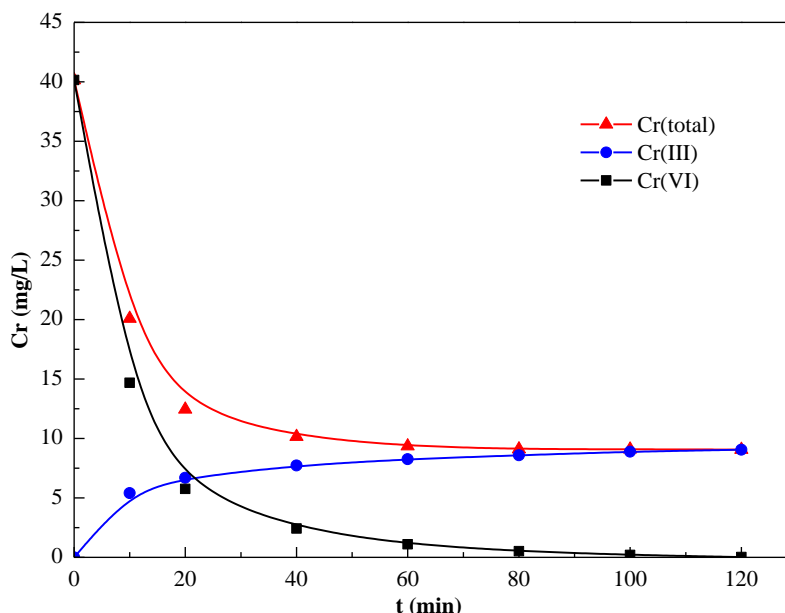


Fig. 15. Adsorption time on the influence of Cr valence state

CONCLUSIONS

1. A Box-Behnken design response surface model was employed for significance analysis, correlation analysis, and variance analysis. The results showed that Cr(VI) initial concentration, dosing quantity, and pH had significant effects on the adsorption. The square of dosing quantity and pH significantly affected the adsorbed amount. The Cr(VI) initial concentration, dosing quantity, and pH showed significant interactions with respect to the adsorption. Analysis of variance showed the model to be highly significant, with good credibility and accuracy. The coefficient of determination R^2 was 0.9875, R_{2Adj} was 0.9714, CV was 0.76%, and the adeq precision was 27.613. The removal rate of Cr(VI) was best when the initial Cr(VI) concentration was 40.2 mg/L, adsorbent dosing quantity was 0.34 g, and reaction pH 2.78. The predicted value was 100.4%, whereas the measured value was 99.998%, showing that the regression equation can reflect actually the influence of various factors.
2. The modified eucalyptus bark was studied for its adsorption process of hexavalent chromium through adsorption isothermal model, adsorption kinetics, and thermodynamics. Results showed that both the Langmuir and Freundlich isothermal models were able to describe the adsorption of Cr(VI). Thus, there was not clear determination as to whether the adsorption of Cr(VI) involved a monolayer with equivalent or heterogeneous surface sites. The adsorption process was found to be a process governed by multiple factors, in which chemical reaction appeared to play a leading role. Thermodynamic parameters $\Delta G^0 < 0$, $\Delta H^0 > 0$, and $\Delta S^0 > 0$ indicate that

the nature of adsorption was spontaneous and endothermic.

3. The mechanism of reaction was further characterized by FTIR, SEM-EDS, and ICP methods. Results showed that redox reactions did take place in the course of the adsorption of Cr(VI). In fact, Cr(III) was the only Cr species remaining in solution at the end of a test carried out under optimized conditions.

ACKNOWLEDGMENTS

The authors thank the Guangxi Key Laboratory of Environmental Pollution Control Theory and Technology for the research assistance. This paper were supported by the Research funds of The Guangxi Key Laboratory of Environmental Engineering, Protection and Assessment (1301K001), the Innovation Project of Guangxi Graduate Education (YCBZ2012003), and the Guangxi Natural Fund (2012GXNSFAA053023 & 2013GXNSFFA019005).

REFERENCES CITED

- Alam, Z., Muyibi, S. A., and Toramae, J. (2007). "Statistical optimization of adsorption processes for removal of 2, 4-dichlorophenol by activated carbon derived from oil palm empty fruit bunches," *J. Environ. Sci.* 19(6), 674-677.
- Aoyama, M., and Tsuda, M. (2001). "Removal of Cr(VI) from aqueous solutions by larch bark," *Wood. Sci. Technol.* 35(5), 425-434.
- Arulkumar, M., Thirumalai, K., Sathishkumar, P., and Palvannan, T. (2012). "Rapid removal of chromium from aqueous solution using novel prawn shell activated carbon," *Chem. Eng. J.* 185-186, 178-186.
- Chen, S., Yue, Q., Gao, B., and Xu, X. (2010). "Equilibrium and kinetic adsorption study of the adsorptive removal of Cr(VI) using modified wheat residue," *J. Colloid Interface Sci.* 349(1), 256-264.
- Garg, U. K., Kaur, M. P., Garg, V. K., and Sud, D. (2007). "Removal of hexavalent chromium from aqueous solution by agricultural waste biomass," *J. Hazard. Mater.* 140(1-2), 60-8.
- Giri, A. K., Patel, R., and Mandal, S. (2012). "Removal of Cr(VI) from aqueous solution by Eichhornia crassipes root biomass-derived activated carbon," *Chem. Eng. J.* 185-186, 71-81.
- Hubbe, M. A., Hasan, S. H., and Ducoste, J. J. (2011). "Cellulosic substrates for removal of pollutants from aqueous systems: A review. 1. Metals," *BioResources* 6(2), 2161-2287.
- Miretzky, P., and Cirelli, A. F. (2010). "Cr(VI) and Cr(III) removal from aqueous solution by raw and modified lignocellulosic materials: A review," *J. Hazard. Mater.* 180(1-3), 1-19.
- Nie, S., Wu, Z., Liu, J., Liu, X., Qin, C., Song, H., and Wang, S. (2013). "Optimization of AOX formation during the first chlorine dioxide bleaching stage (D₀) of soda AQ bagasse pulp," *Appita J.* 66(4), 306-312.
- Saha, R., Nandi, R., Saha, B. (2011). "Sources and toxicity of hexavalent chromium," *J. Coord. Chem.* 64(10), 1728-1806.

- Saha, R., Saha, I., Nandi, R., Ghosh, A., Basu, A., Ghosh, S. K., and Saha, B. (2013). "Application of chattim tree (devil tree, *Alstonia scholaris*) saw dust as a biosorbent for removal of hexavalent chromium from contaminated water," *Can. J. Chem. Eng.* 91(5), 814-820.
- Saha, B., and Orvig, C. (2010). "Biosorbents for hexavalent chromium elimination from industrial and municipal effluents," *Coord. Chem. Rev.* 254, 2959-2972.
- Saha, R., and Saha, B. (2014). "Removal of hexavalent chromium from contaminated water by adsorption using mango leaves (*Mangifera indica*)," *Des. Wat. Treat.* 52(10-12), 1928-1936.
- Sahu, J. N., Acharya, J., and Meikap, B. C. (2009). "Response surface modeling and optimization of chromium(VI) removal from aqueous solution using tamarind wood activated carbon in batch process," *J. Hazard. Mater.* 172(2-3), 818-25.
- Sarin, V., and Pant, K. K. (2006). "Removal of chromium from industrial waste by using eucalyptus bark," *Bioresour. Technol.* 97(1), 15-20.
- Şengil, İ. A., Özacar, M., and Türkmenler, H. (2009). "Kinetic and isotherm studies of Cu(II) biosorption onto valonia tannin resin," *J. Hazard. Mater.* 162(2), 1046-1052.
- Shojaimehr, T., Rahimpour, F., Khadivi, M. A., and Sadeghi, M. (2014). "A modeling study by response surface methodology (RSM) and artificial neural network (ANN) on Cu²⁺ adsorption optimization using light expended clay aggregate (LECA)," *J. Ind. and Eng. Chem.* 20(3), 870-880.
- Wang, X. S., Li, Z. Z., and Sun, C. (2008). "Removal of Cr(VI) from aqueous solutions by low-cost biosorbents: Marine macroalgae and agricultural by-products," *J. Hazard. Mater.* 153(3), 1176-1184.
- Zhang, Z., Peng, J., Srinivasakannan, C., Zhang, Z., Zhang, L., Fernández, Y., and Menéndez, J. (2010). "Leaching zinc from spent catalyst: Process optimization using response surface methodology," *J. Hazard. Mater.* 176(1), 1113-1117.

Article submitted: July 24, 2014; Peer review completed: September 24, 2014;

Revised version received and accepted: September 28, 2014; Published: October 6, 2014.